

Design Aid of Semi-rigid Connections for Frame Analysis

N. KISHI, W. F. CHEN, Y. GOTO, and K. G. MATSUOKA

ABSTRACT

In this paper, a useful design aid for determining the values of the initial connection stiffness R_{ki} , the ultimate moment capacity M_u , and the shape parameter n of a three-parameter power model describing the moment-rotation curve ($M-\theta_r$) of semi-rigid connections with angles is prepared for its use in the practical design of flexibly jointed frames with angles. A set of nomographs allows the engineer to rapidly determine the $M-\theta_r$ curve for a given connection.

Applying the design aid, numerical simulations on drift and column moment of a flexibly jointed frame with angles are illustrated.

1. INTRODUCTION

The aim of the work described in this paper is to provide a practical procedure for the analysis and design of semi-rigid frames with angles. To this end, a set of nomographs allows the engineer to determine rapidly the values of the initial connection stiffness R_{ki} , the ultimate moment capacity M_u , and the shape parameter n of a three-parameter power model describing the $M-\theta_r$ curve of connections. In this development, a data base of steel beam-to-column connections was first built and simple procedures to enable engineers to assess this $M-\theta_r$ behavior were then formulated. Using this data base, extensive comparisons were made with the results of tests on actual connections providing final confirmation of the validity of the three-parameter power model. The model is recommended for general use in semi-rigid frame analysis.

In this paper, we have established a design procedure for connections with angles. The three-parameter power model is adopted to represent the nonlinear $M-\theta_r$ curve proposed

previously by Richard and Abbott (1975). The three parameters in this model are the initial connection stiffness R_{ki} , the ultimate moment capacity of connection M_u , and the shape parameter n . The values of R_{ki} and M_u can be determined by a simple mechanical procedure with an assumed failure mechanism (Kishi and Chen, 1990). Herein, we prepared a useful design aid for the values of these parameters corresponding to given angles and beam, or the main parameters of connection angles for given values of R_{ki} and M_u . The shape parameter n can be determined as a linear function of $\log_{10}\theta_0$ (Kishi and Chen et al. 1991) which is an empirical equation based on experimental data installed in the Program SCDB (Chen and Kishi 1989), where $\theta_0=M_u/R_{ki}$.

Using the nomographs for R_{ki} and M_u and the empirical equation for n , we can determine rapidly the nonlinear $M-\theta_r$ curve of connections with angles. Then, using the second-order elastic analysis program FRAME formulated by Goto and Chen (1987), we can analyze the flexibly jointed frame in a simple manner (Chen and Lui, 1991). As an illustrative example, studies of a four-bay, two-story frame with variable beam section and/or length or thickness of connection angles made using this analysis are presented.

2. ASSUMPTIONS AND NOTATIONS

In this paper, four types of connections with angles are considered: single/double web-angle connections and top-and-seat-angle with/without double web-angle connections as shown in Figures 1 to 3. To prepare the design charts for the initial connection stiffness R_{ki} and the ultimate moment capacity M_u , the dimensions used for angle as shown in Figure 4 are defined as:

- t = angle thickness
- k = gauge distance from heel to the top of fillet
- l = angle length
- g = distance between heel to the center of fastener closest to web or flange of beam
- W = nut width
- $I_0 = t^3 / 12$ = geometrical moment of inertia
- $M_0 = \sigma_y t^2 / 4$ = pure plastic bending moment

where σ_y is the yielding stress of steel, and I_0 and M_0 the values per unit length of plate element of angle. We assume that top angle and seat angle have the same dimensions.

N. Kishi is associate professor, civil engineering, Muroran Institute of Technology, Muroran, Japan 050.

W. F. Chen is George E. Goodwin distinguished professor of civil engineering and head of structural engineering, School of Civil Engineering, Purdue University, West Lafayette, IN.

Y. Goto is professor, civil engineering, Nagoya Institute of Technology, Nagoya, Japan 466.

K. G. Matsuoka is professor, civil engineering, Muroran Institute of Technology, Muroran, Japan 050.

Furthermore, we shall introduce the following non-dimensional parameters:

$$\beta = \frac{g}{l}, \gamma = \frac{l}{t}, \delta = \frac{d}{t}, \kappa = \frac{k}{t}, \omega = \frac{W}{t}, \rho = \frac{t_w}{t_t}$$

in which d is the height of beam and subscripts "t" and "w" denote top angle and web angle respectively.

3. CHARTS FOR R_{ki} and M_u IN CONNECTIONS WITH ANGLES

To prepare the charts for the initial connection stiffness R_{ki} and the ultimate moment capacity M_u , the equations developed previously by Kishi and Chen (1990) are used. All charts are basically related to the parameter β . Extensive

comparisons of the analytical solutions with experimental test results can be found in the paper by Kishi and Chen (1990).

3.1 Single/Double Web-Angle Connections

Using a simple mechanical procedure described in the paper cited above, the values of R_{kiw} and M_u for single web-angle connections are formulated as:

$$\frac{R_{kiw}}{EI_{0w}} = \frac{12\alpha \cos h(\alpha\beta_w')}{7.8\{(\alpha\beta_w') \cos h(\alpha\beta_w') - \sin h(\alpha\beta_w')\}} \quad (1)$$

$$\frac{M_{uw}}{M_{0w}t_w} = \frac{(2\xi_w + 1)}{3} \gamma_w^2 \quad (2)$$

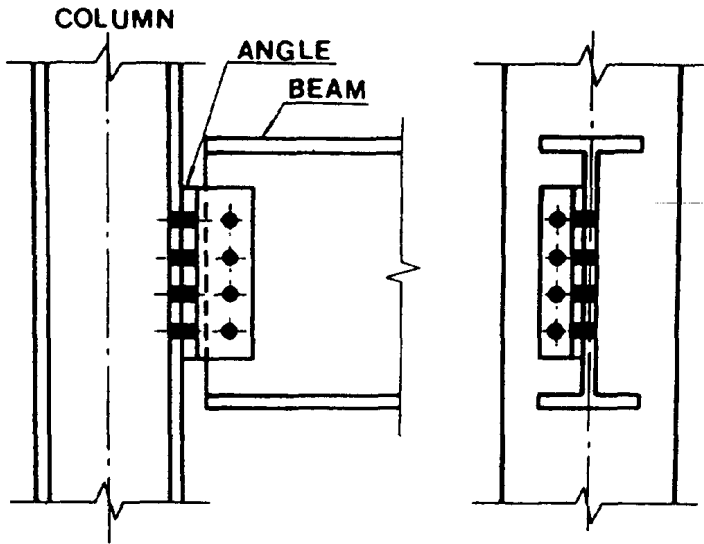


Fig. 1. Single web-angle connections.

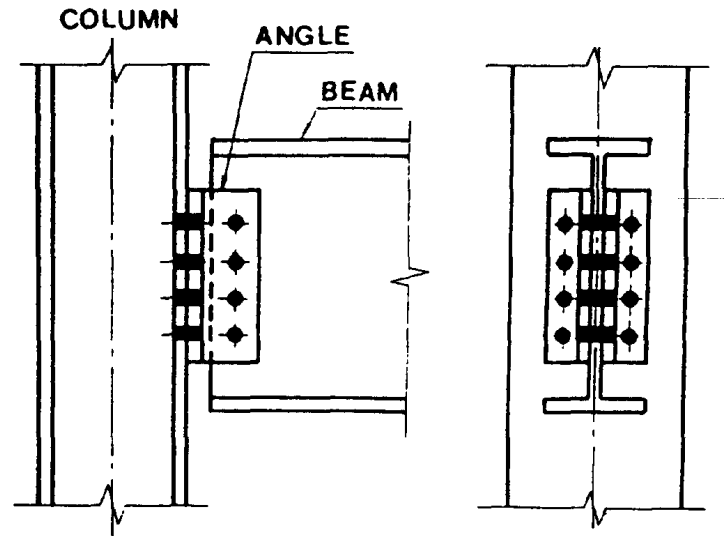
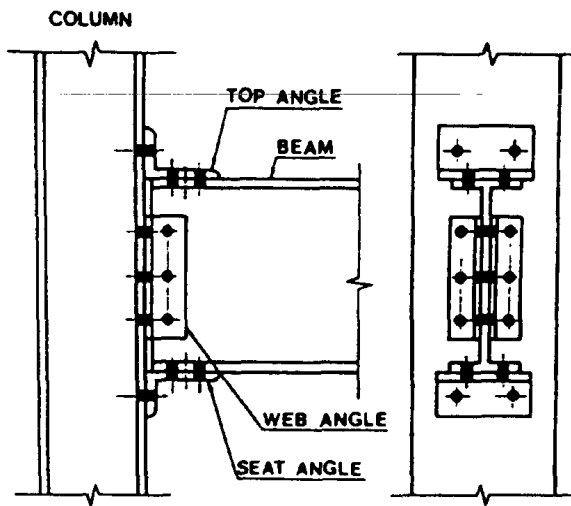
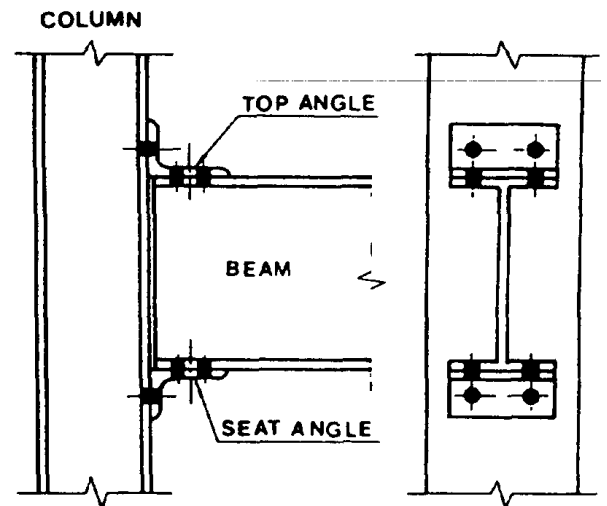


Fig. 2. Double web-angle connections.



(a) Top and seat angle with double web-angle connection



(b) Top and seat angle without double web-angle connection

Fig. 3. Top and seat angle with/without double web-angle connections.

in which $\alpha=4.2967$ and β_w' is defined as

$$\beta_w' = \beta_w - \frac{1}{\gamma_w} \left(\kappa_w + \frac{\omega_w}{2} \right) \quad (3)$$

ξ_w in Equation 2 is obtained by solving Equation 4 which is derived by combining the Drucker interaction equation between bending moment and shearing force with the Tresca yielding criterion as

$$\xi_w^4 + (\beta_w \gamma_w - \kappa_w) \xi_w - 1 = 0 \quad (4)$$

The non-dimensional initial connection stiffness as a function of β_w' for single web-angle connections is shown in

Figure 5. The non-dimensional ultimate connection moment is shown in Figure 6 in which β_w is taken as abscissa and γ_w is varied from 5 to 20 with an increment of 5 for $\kappa_w = 1.5$ and 2.0.

The case of double web-angle connections can be obtained simply by doubling the values found from these charts.

3.2 Top and Seat Angle Without Double Web-Angle Connection

Assuming that the center of rotation is located at the angle leg adjacent to the compression beam flange and the top angle acts as a cantilever beam to resist surcharged moment, the initial connection stiffness R_{kts} is obtained as (Kishi and Chen, 1990).

$$\frac{R_{kts}}{EI_{0t}} = (1 + \delta_t)^2 D_{ts} \quad (5)$$

in which D_{ts} is a function of β_t' and γ_t and those D_{ts} and β_t' are given by

$$D_{ts} = \frac{3}{\beta_t' (\gamma_t^2 \beta_t'^2 + 0.78)} \quad (6)$$

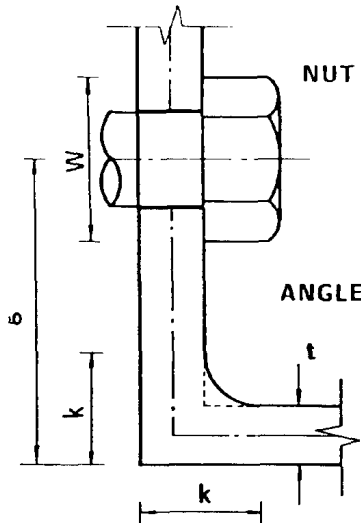


Fig. 4. Main parameters for an angle.

$$\beta_t' = \beta_t - \frac{(1 + \omega_t)}{2\gamma_t} \quad (7)$$

The ultimate moment capacity M_{uts} is obtained by assuming a simple failure mechanism. The equation for M_{uts} is given by

$$\frac{M_{uts}}{M_{0t} t_t} = \gamma_t \left\{ 1 + \xi_t (1 + \beta_t^* + 2(\kappa_t + \delta_t)) \right\}$$

where the variable ξ_t is a non-dimensional ultimate shearing force acting at the plastic hinge. Here, as in the case of single

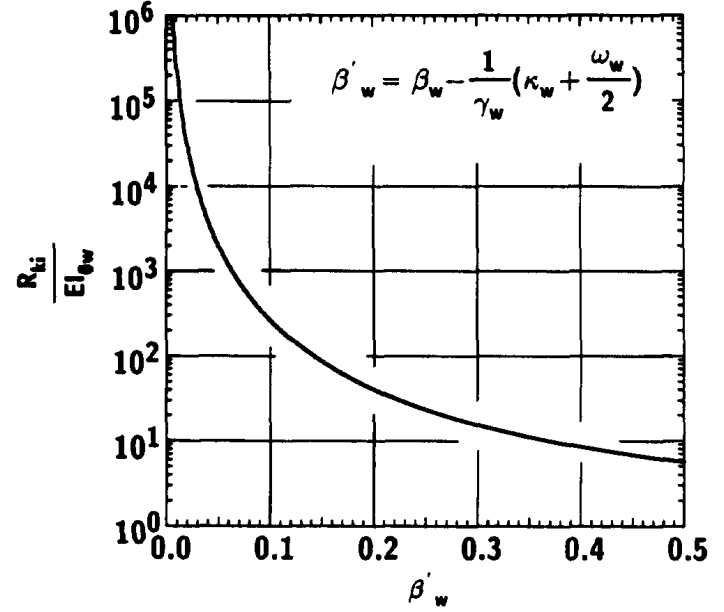


Fig. 5. Initial connection stiffness for single web-angle connections.

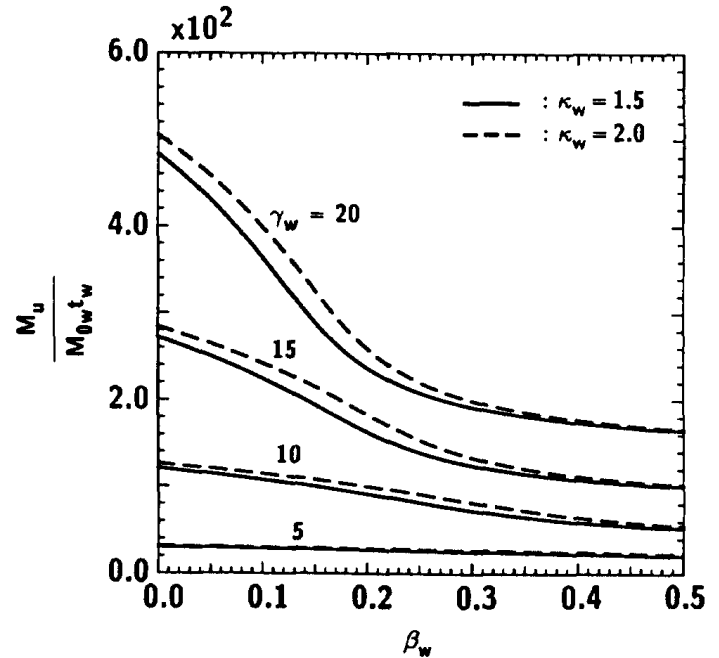


Fig. 6. Ultimate moment capacity for single web-angle connections.

web-angle connections, it is obtained by solving Equation 9 as

$$\xi_t^4 + \beta_t^* \xi_t - 1 = 0 \quad (9)$$

in which β_t^* is defined as

$$\beta_t^* = \beta_t' \gamma_t - \kappa_t \quad (10)$$

The distributions of the coefficient D_{ts} for R_{kits} with respect to β_t' are shown in Figure 7 in which γ_t is varied from 5 to 40 with an increment of 5. Figure 8 is the chart for the non- with the dimensional ultimate moment capacity M_{uts} . Figure 8(a) shows the results variation of γ_t for $\delta_t = 40$ and 80, while Figure 8(b) shows the variation of δ_t (10 to 80) for $\gamma_t = 5$ and 40.

3.3 Top and Seat Angle With Double Web-Angle Connection

In this type of connection, the initial connection stiffness R_{ki} and the ultimate moment capacity M_u can be evaluated by separating the top- and seat-angle part and the double web-angle part as

$$\frac{R_{ki}}{EI_{0t}} = \frac{R_{kits}}{EI_{0t}} + \frac{R_{kiw}}{EI_{0t}}, \quad \frac{M_u}{M_{0t}t_t} = \frac{M_{uts}}{M_{0t}t_t} + \frac{M_{uw}}{M_{0t}t_t} \quad (11,12)$$

Since the top- and seat-angle part of the equations derived above are also applicable for the case of the top- and seat-angle connections, Figure 7 can be used for R_{kits}/EI_{0t} and Figure 8 for $M_{uts}/M_{0t}t_t$ in this type of connections.

As for the web angle, it acts as a cantilever beam similar to the behavior of the top angle, the initial connection

stiffness R_{kiw} is related to the double web-angle connection part as (Kishi and Chen, 1990)

$$\frac{R_{kiw}}{EI_{0t}} = (1 + \delta_t)^2 \rho D_w \quad (13)$$

in which D_w is

$$D_w = \frac{3}{2\beta_w'(\gamma_w^2 \beta_w'^2 + 0.78)} \quad (14)$$

where β_w' is defined the same as β_t' in Equation 7.

In the limit state, choosing a simple failure mechanism of web angle and taking moment about the center of rotation at the angle leg adjacent to the compression beam flange, the ultimate moment capacity M_{uw} is

$$\frac{M_{uw}}{M_{0t}t_t} = \gamma_w(1 + \xi_w) \left\{ \frac{\xi_w - 1}{3(\xi_w + 1)} \gamma_w + \delta_w + \frac{1}{\rho} \right\} \rho^3 \quad (15)$$

in which ξ_w is obtained by solving Equation 4, since the mechanism assumed here is the same as in the single web-angle connections.

The distributions of the coefficient D_w for R_{kiw}/EI_{0t} are given in Figure 9. M_{uw} has a total of five variables: $\beta_w, \delta_w, \gamma_w, \rho$, and κ_w . Taking β_w as abscissa, two types of charts are prepared in this study. In the first case, γ_w is varied from 5 to 35 and/or 40 with an increment of 5 while the values of δ_w, ρ , and κ_w are kept constant (Figure 10). In the second case, δ_w instead of γ_w is varied in a similar manner (Figure 11). Though it is easy to obtain these curves for arbitrary values of these parameters, we consider here only two cases $\rho = 0.5$ or 1.0 and $\kappa_w = 1.5$ or 2.0.

4. DETERMINATION OF $M-\theta_r$ CURVE OF CONNECTION

It is a simple matter to obtain the values of R_{ki} and M_u for given dimensions of angle or to determine the angle dimensions for given values of R_{ki} and M_u . Moreover, we must also determine the nonlinear characteristics of connection behavior for a structural analysis (Chen, 1987). The three-parameter power model is adopted here to represent these characteristics of semi-rigid connections which is a simplification of the four-parameter power model proposed previously by Richard and Abbott (1975).

Assuming $m = M / M_u$, $\theta = \theta_r / \theta_0$ and $\theta_0 = M_u / R_{ki}$ and introducing the shape parameter n , the power model used here has the simple form

$$m = \frac{\theta}{(1 + \theta^n)^{1/n}} \quad (16)$$

Figure 12 shows the $M-\theta_r$ curves of a connection with several values of shape parameter n . In one extreme, if the shape parameter n is taken to be infinity, the model reduces to a bilinear curve with the initial connection stiffness R_{ki} and

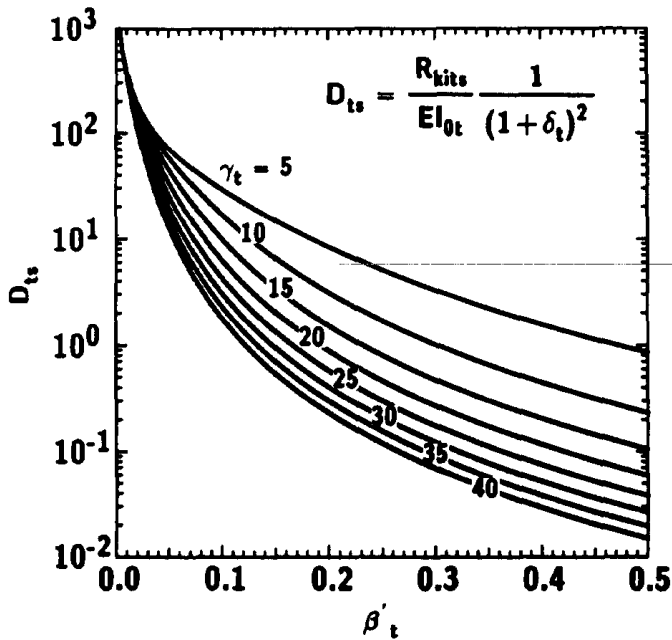
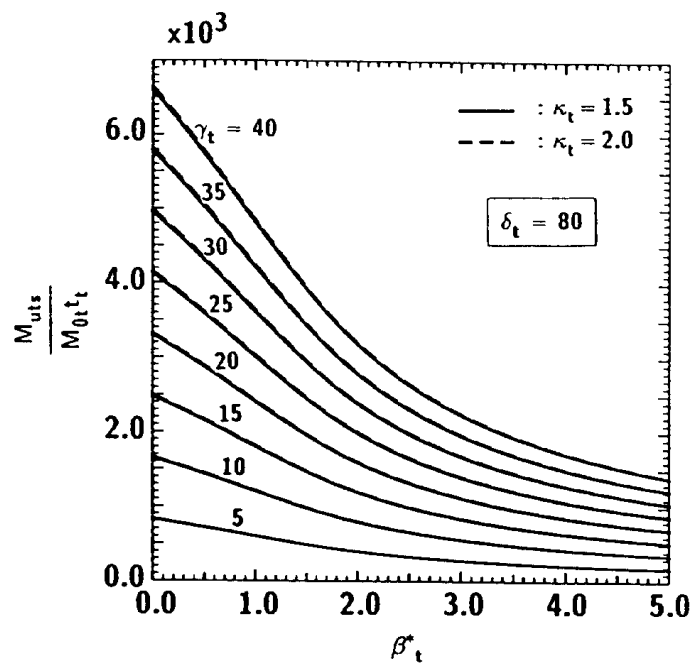
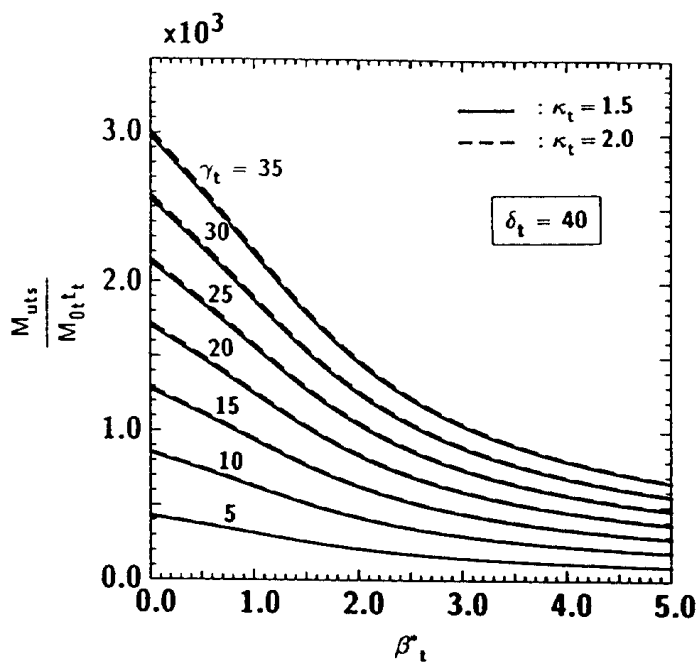
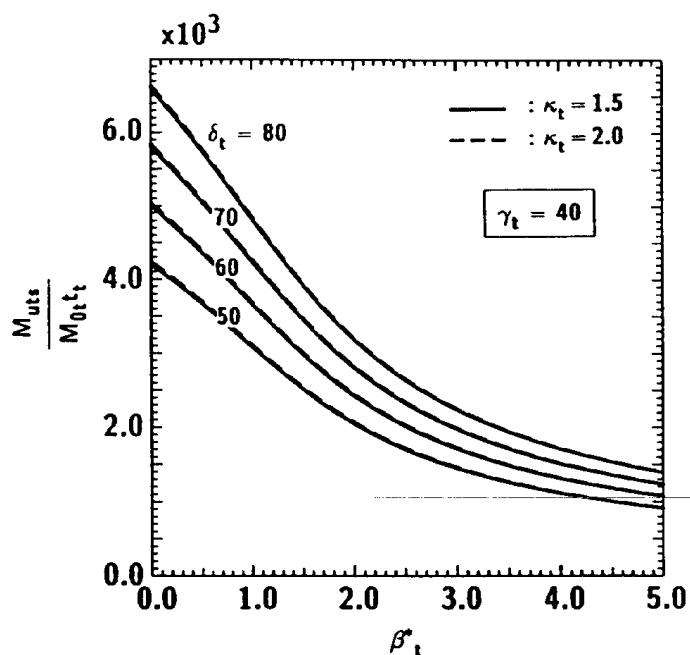
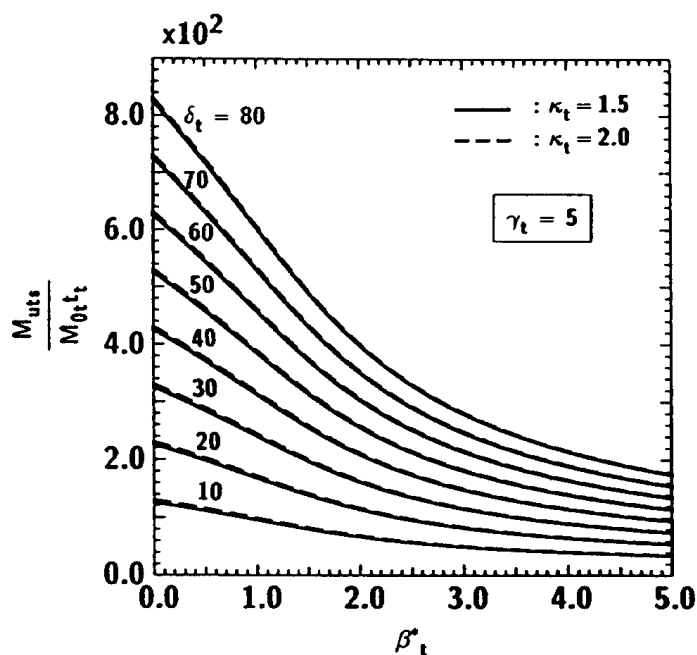


Fig. 7. Coefficient D_{ts} for R_{kits} of top and seat angle without double web-angle connections.



(a) Varying γ_t for $d_t=40$ and 80



(b) Varying d_t for $g_t=5$ and 40

Fig. 8. Ultimate moment capacity for top and seat angle without double web-angle connections.

Table 1. Empirical Equations for Shape Parameter n		
Type No.	Connection Type	n
I	Single web-angle connection	$0.520 \log_{10} \theta_0 + 2.291$ 0.695 ... $\log_{10} \theta_0 > -3.073$ ≤ -3.073
II	Double web-angle connection	$1.322 \log_{10} \theta_0 + 3.952$ 0.573 ... $\log_{10} \theta_0 > -2.582$ ≤ -2.582
III	Top- and seat-angle connection (with double web angle)	$1.398 \log_{10} \theta_0 + 4.631$ 0.827 ... $\log_{10} \theta_0 > -2.721$ ≤ -2.721
IV	Top- and seat-angle connection (with double web angle)	$2.003 \log_{10} \theta_0 + 6.070$ 0.302 ... $\log_{10} \theta_0 > -2.880$ ≤ -2.880

the ultimate moment capacity M_u . The principal merit of the present model is a significant saving of computing time in a non-linear structural analysis program, since the connection moment M can be represented as a function of relative rotation θ_r . Furthermore, the tangent connection stiffness R_k can be directly obtained without iteration.

As for the shape parameter n , we use the following procedure for its determination (Kishi and Chen et al. 1991):

1. The shape parameter n for each experimental test data is numerically determined first by the least mean square technique of the test data with Equation 16.
2. The shape parameter is assumed to be a linear function of $\log_{10} \theta_0$. Using a statistical technique for n values obtained from the above procedure, empirical equation for n for each connection type are determined.

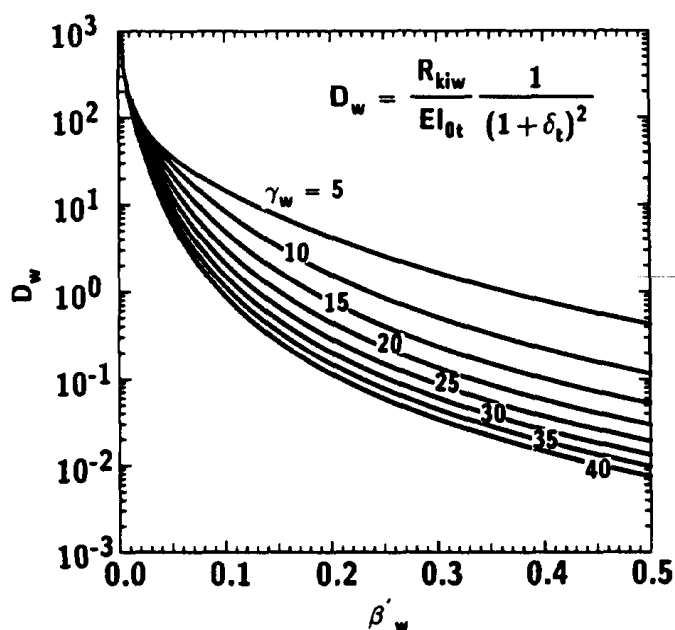


Fig. 9. Coefficient D_w for R_{kiw} / EI_{0t} of top and seat angle with double web-angle connections.

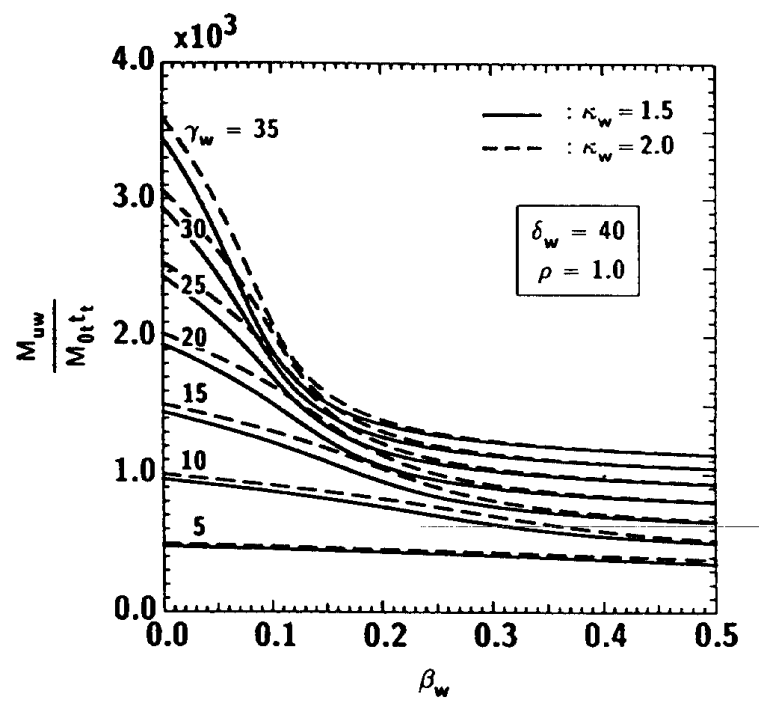
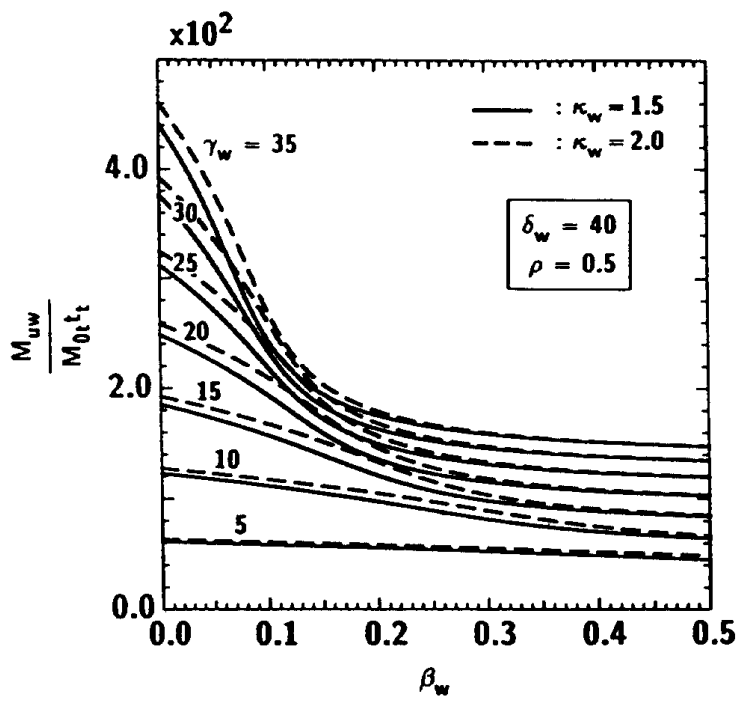
Figure 13 shows comparisons of the distributions of n values of the empirical equation with the experimental test data installed in the program SCDB (Kishi and Chen, 1989). From these numerical considerations, we conclude that within the current practice of the range of the connection variables, the three-parameter power model with the shape parameter n obtained from the empirical equation can be applied in practical design (Kishi and Chen et al. 1991). In this study, we set the shape parameter n to be constant for the region of θ_0 less than the smallest one obtained from experimental test data. The equation refined for each connection type is listed in Table 1.

5. NUMERICAL EXAMPLE OF STRUCTURAL ANALYSIS OF FLEXIBLY JOINTED FRAME

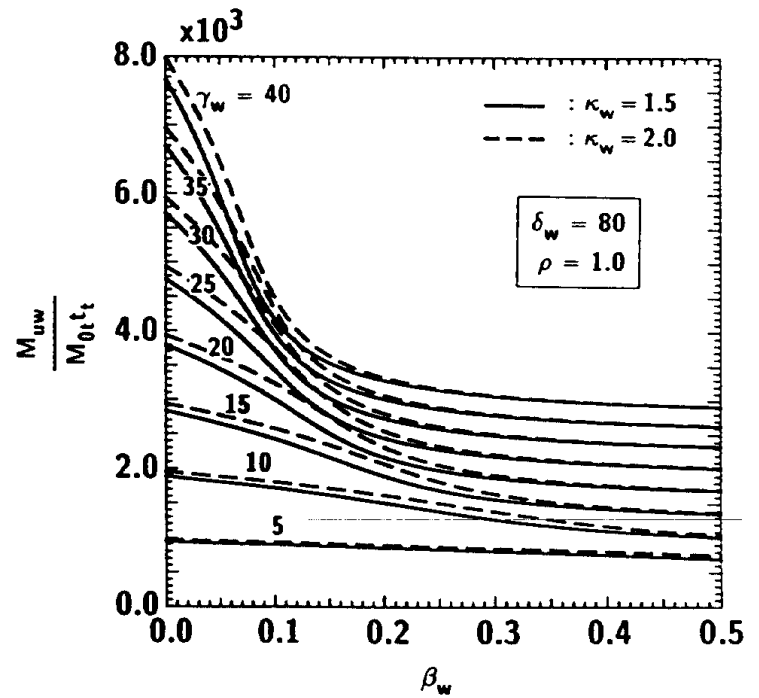
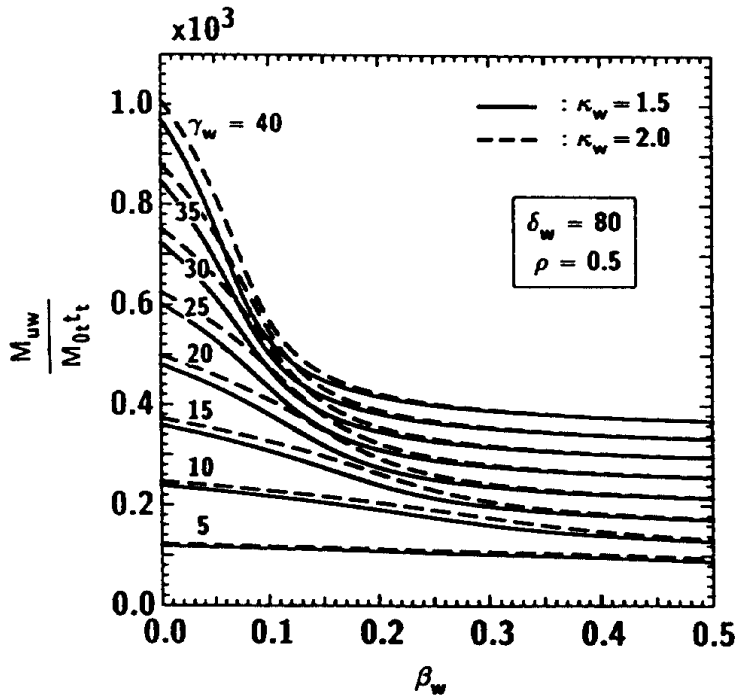
In this study, a four-bay, two-story frame used by Lindsey (1987) is taken as the frame of basic skeleton for the present numerical analysis (Figure 14).

W8×24 and W8×31 sections are used as the external and internal columns respectively and the frames are placed 25 ft center to center. The loads are: floor dead load: 65 psf, roof dead load: 20 psf, reduced floor live load: 40 psf, and roof live load: 12 psf. Wind loads are assumed to be 15 psf with a shape factor of 1.3. Two types of load combination are considered referring to AISC-LRFD specification (1986). One is the unfactored loads ($D+L+W$) to check the drift under service load. Another is the factored loads ($1.2D + 0.5L + 1.3W$) to check the frame stability. Load intensities are $W_R=0.80$ k/ft, $W_F=2.70$ k/ft, $P_R=2.925$ kip, $P_F=6.581$ kip for the unfactored loads and $W_R=0.75$ k/ft, $W_F=2.54$ k/ft, $P_R=3.803$ kip, $P_F=8.556$ kip for the factored loads.

In the present study, we adopt the top and seat angle with double web-angle connections as a part of the beam-to-column connection. The combinations of beam, column, and connection angle for several cases are listed in Table 2 in which the size of the columns is constant for each case. Beams used in Cases 1 and 2 are stronger than those in Cases 3 and 4. Heavy hex structural bolts with 1-in. nominal size are used as

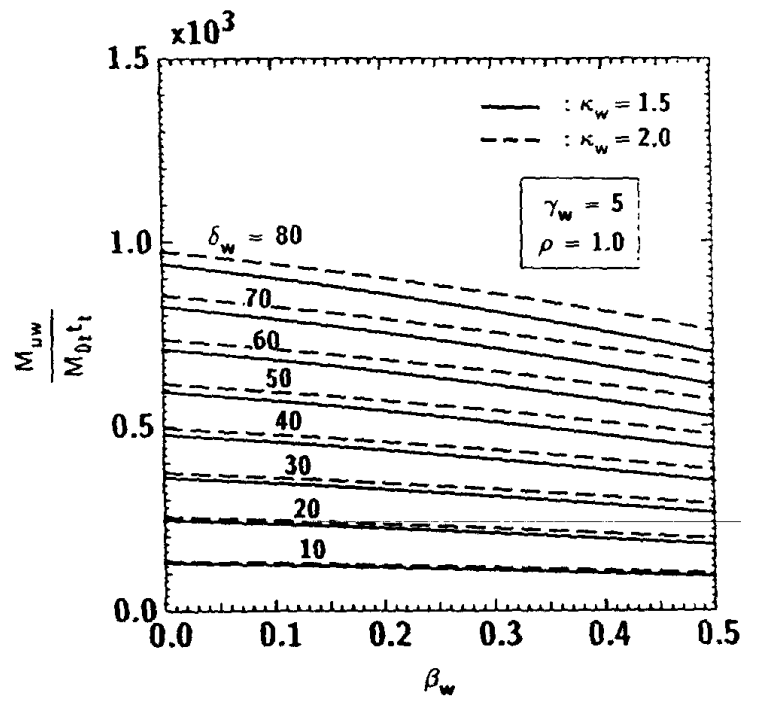
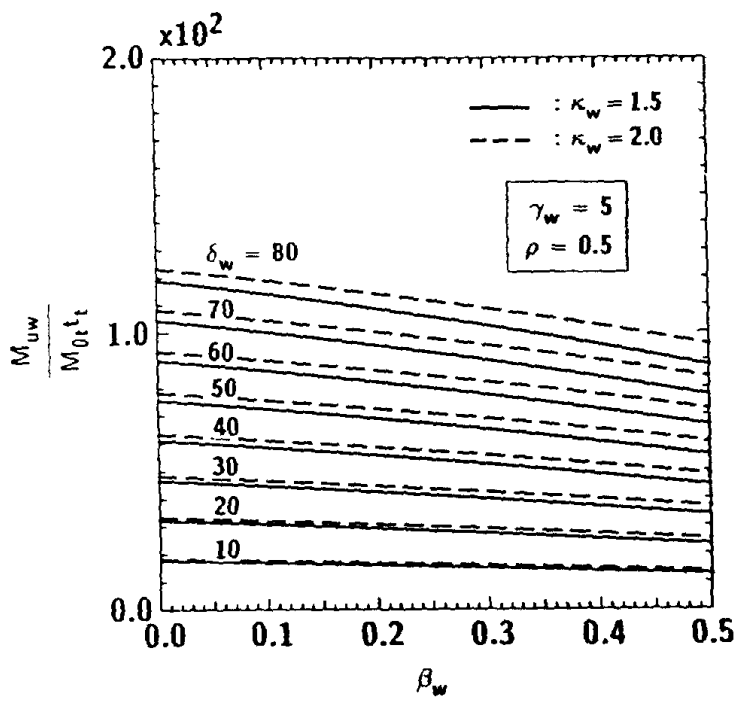


(a) $r=0.5$ and 1.0 for $d_w=40$

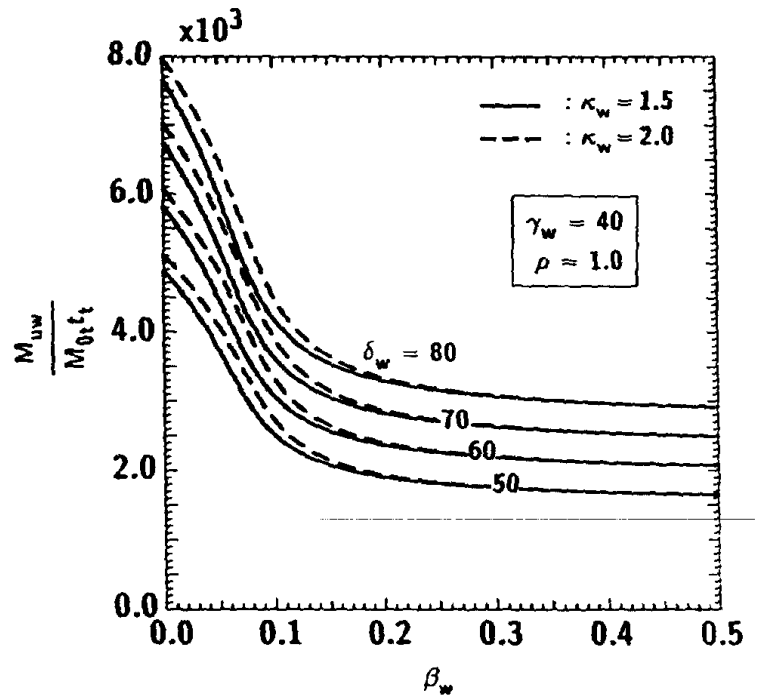
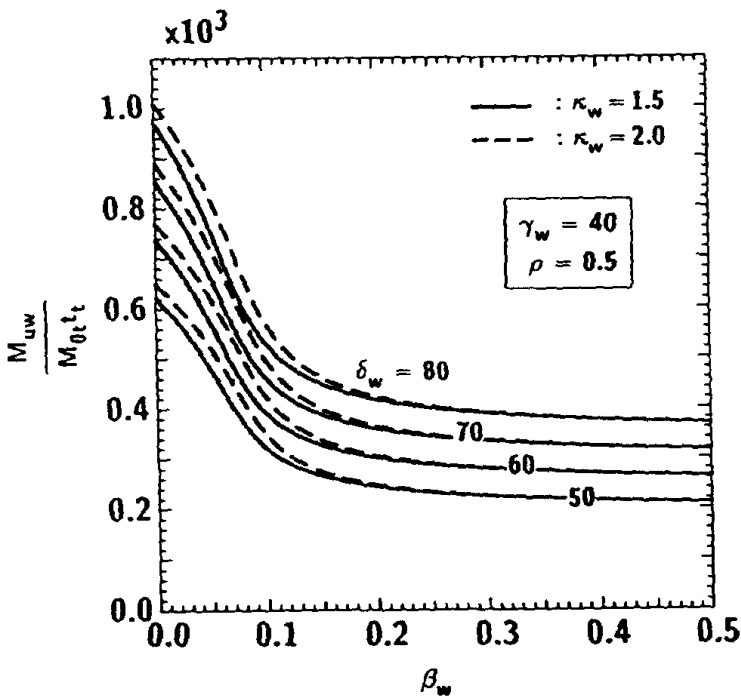


(b) $r=0.5$ and 1.0 for $d_w=80$

Fig. 10. Ultimate moment for the variation of β_w for top and seat angle with double web-angle connections.



(a) $r=0.5$ and 1.0 for $g_w=5$



(b) $r=0.5$ and 1.0 for $g_w=40$

Fig. 11. Ultimate moment for the variation of d_w for top and seat angle with double web-angle connections.

Table 2. Combinations of Beam, Column, and Connection Angles					
Beam and Column Sizes:					
	Case 1, 2			Case 3, 4	
Floor beam	W18×50			W18×46	
Roof Beam	W14×22			W12×19	
Extetal column	W8×24			W8×24	
Internal column	W8×31			W8×31	
Top- and Seat-Angle Sizes:					
	Size	<i>l</i>	<i>g</i>	<i>l</i>	<i>g</i>
T & S Angles	L4×3½× <i>t_t</i>	6 in.	var.	var.	2.5 in.
Web Angles	L3×2½×¼	8.5 in. for floor 5.5 in. for roof	1.75 in.	8.5 in. for floor 5.5 in. for roof	1.75 in.

fasteners for all cases.

6. NUMERICAL RESULTS

6.1 Characteristics of $M-\theta_r$ Curve of Connections

The $M-\theta_r$ curves of connections used are shown in Figure 15 in which the dimensions of beams and angles are specified in Case 1 and the length of top and seat angles is six inches.

6.2 Drift of Frame in Case Surcharging Unfactored Loads

The general configurations of deformation of flexibly jointed frame under the service loads are shown in Figure 16 comparing with the results of rigid connections, in which the sections of members are taken as $l_t = 6$ in. and $t_t = \frac{1}{4}$ -in. and/or $\frac{1}{2}$ -in. as in Cases 2 and 4. Though R_{ki} and M_u in the case of $t_t = \frac{1}{2}$ -in. may be twice than that of $t_t = \frac{1}{4}$ -in. as we can see in Figure 15, the drift of roof in the case of $t_t = \frac{1}{4}$ -in. is less than twice that of $t_t = \frac{1}{2}$ -in. The drifts for $t_t = \frac{1}{2}$ -in. and $\frac{1}{4}$ -in. are almost two to three times than that of

the result of rigid connections, respectively.

Distributions of the non-dimensional roof drift (Δ / H) for each case are shown in Figure 17 taking l_t or g_t as abscissa in which Δ and H are roof drift and height of frame respectively. From this figure, we can select some dimensions for top and seat angles for a given drift. For example, if the maximum drift is set to be $\Delta / H = 1/300$, we can choose three types of angles to meet this requirement as

For Cases 1 and 2:

$$t_t = \frac{1}{2}\text{-in.} \quad g_t = 2.75 \text{ in.} \quad l_t = 6 \text{ in.}$$

and

$$t_t = \frac{1}{2}\text{-in.} \quad g_t = 2.50 \text{ in.} \quad l_t = 5 \text{ in.}$$

For Cases 3 and 4:

$$t_t = \frac{1}{2}\text{-in.} \quad g_t = 2.50 \text{ in.} \quad l_t = 6 \text{ in.}$$

6.3 Frame Stability in Case Surcharging Factored Loads

Bending moment diagrams of the frame in Cases 2 and 4 with $l_t = 6$ in. and $t_t = \frac{1}{4}$ -in. and/or $\frac{1}{2}$ -in. under the factored loads are shown in Figure 18 together with the results of rigid connections. The bending moments on floor beams show a large difference between the semi-rigid and rigid connections. On the other hand, the differences on other members are smaller than those of the floor beams.

The non-dimensional end moments of columns of Cases 1 to 4 are tabulated in Table 3 together with the results of rigid connections and the B_1 , B_2 method as given in AISC-LRFD specification (Chen and Lui, 1987). The reference values in each case are obtained from a first order elastic analysis with rigid connections. In these tables, all values at the fixed points of flexibly jointed frame in all cases are greater than the reference value, and its maximum value is almost 3.5

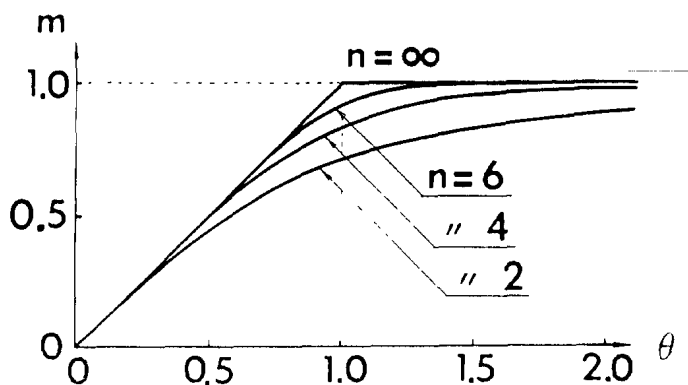
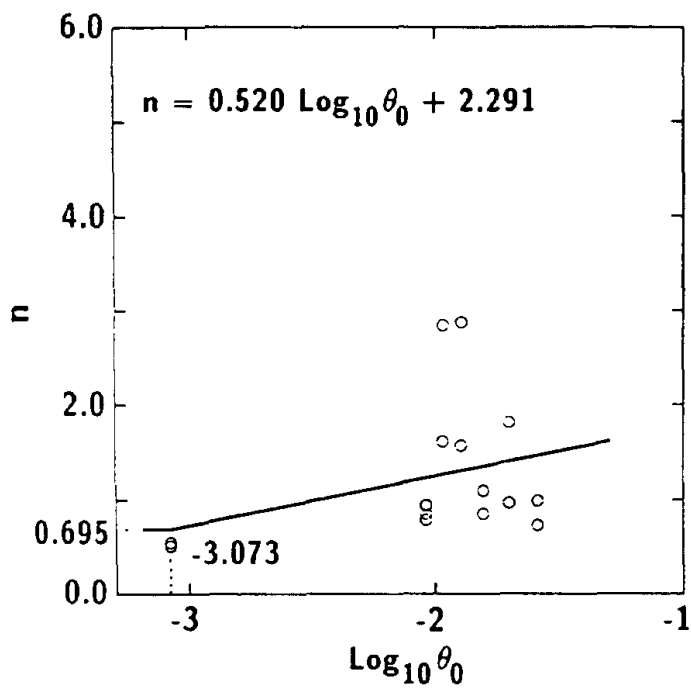
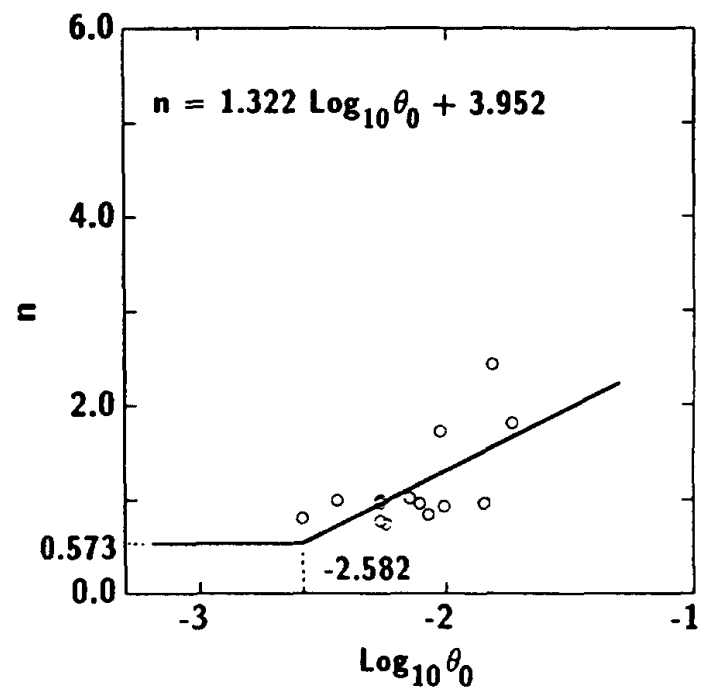


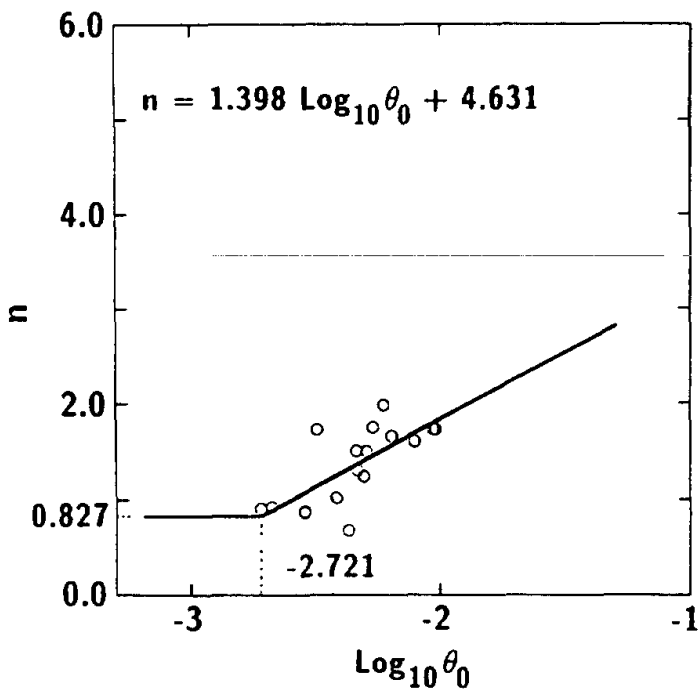
Fig. 12. $M-\theta_r$ curves for the three-parameter power model.



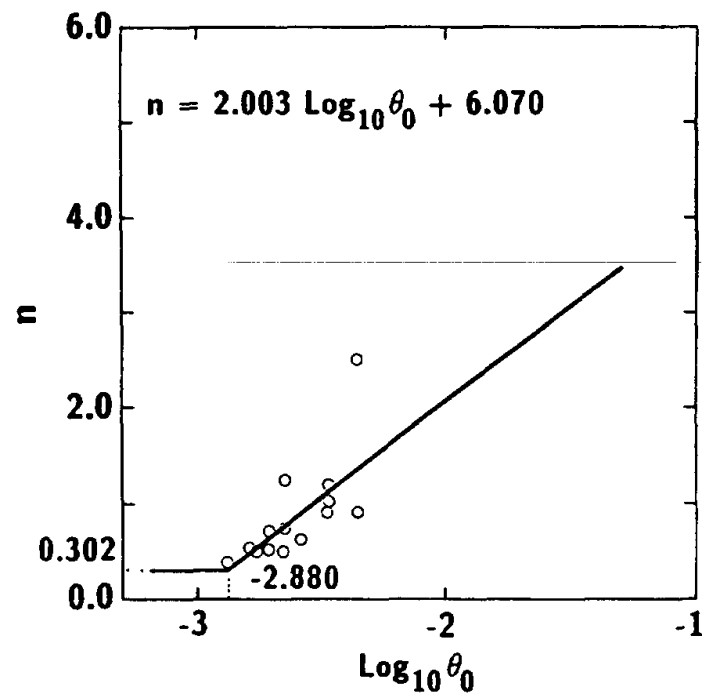
(a) Single Web-angle Connections



(b) Double Web-angle Connections



(c) Top- and Seat-angle with
Double Web-angle Connections



(d) Top- and Seat-angle without
Double Web-angle Connections

Fig. 13. Comparison of the shape parameter n of the empirical equation with experimental test data.

On the other hand, referring to the results of rigid connections, it is clear that the values (1) obtained from the

7. SUMMARY AND CONCLUSIONS

A considerable amount of test data on semi-rigid connections with angles has been collected and analyzed and simple models developed in the past years. Against the background

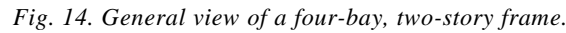


Fig. 15. M - θ_r curves of connections in Case 1.

of this information, design aids for a three-parameter connection model put forward recently by Kishi and Chen is prepared here. A set of nomographs allows the engineer to rapidly determine the values of initial connection stiffness R_{ki} and the ultimate moment capacity M_u for a given connection, or the basic dimensions of angles for given values of R_{ki} and M_u . The general validity of the design procedures based on these developed design charts is demonstrated by comparisons with computed displacements and moments at service loads and factored loads of a four-bay, two-story frame with semi-rigid connections using a second-order elastic analysis program. With the aid of these design charts, the present analysis procedure for the design of semi-rigid frames with angles has achieved both simplicity in use and, as far as possible, a realistic representation of actual behavior. Taking this point in conjunction with the demonstrated validity of the approach, it is recommended for general use.

REFERENCES

1. American Institute of Steel Construction, *Load and Resistance Factor Design Specification for Structural Buildings*, Chicago, IL, 1986.
2. Chen, W. F., editor, "Joint Flexibility in Steel Frames", *Journal of Construction Steel Research*, Special Issue, Vol. 8, Elsevier Applied Science, London, 290 pp, 1987.
3. Chen, W. F. and Lui, E. M., *Structural Stability: Theory and Implementation*, Elsevier, New York, 486 pp, 1987.
4. Chen, W. F. and Lui, E. M., *Stability Design of Steel Frames*, CRC Press, Boca Raton, Florida, 380 pp, 1991.
5. Chen, W. F. and Kishi, N., "Semi-Rigid Steel Beam-to-Column Connections: Data Base and Modeling," *ASCE Journal Structural Engineering*, 115(ST1), pp. 105–119, 1989.
6. Goto, Y. and Chen, W. F., "On the Computer-Based Design Analysis for Flexibly Jointed Frames," *Journal of Construction Steel Research*, 8, pp. 203–231, 1987.
7. Kishi, N. and Chen, W. F., "Data Based of Steel Beam-to-Column Connections," *Structural Engineering Report No. CE-STR-80-26*, School of Civil Engineering, Purdue University, West Lafayette, IN, 653 pp, 1986.
8. Kishi, N. and Chen, W. F., "Moment-Rotation Relations of Semi-Rigid Connections with Angles," *ASCE Journal Structural Engineering*, 116(ST7), pp. 1813–1834, 1990.
9. Kishi, N., Chen, W. F., Goto, Y. and Matsuoka, K. G. "Applicability of Three-Parameter Power Model to Structural Analysis of Flexibly Jointed Frames," *ASCE Mechanics Computing in 1990s and Beyond*, pp. 238–242, 1991.
10. Lindsey, S. D. "Design of Frames with PR Connections," *Journal of Construction Steel Research*, 8, pp. 251–260, 1987.
11. Richard, R. M. and Abbott, B. J., "Versatile Elastic-Plastic Stress-Strain Formula," *ASCE Journal Engineering Mechanical Division*, Vol. 101, No. EM4, pp. 511–515, 1975.

NOMENCLATURE

d	beam depth
D_{ts}	defined in Equation 6
D_w	defined in Equation 14
g	distance between heel to the center of fastener closest to web or flange of beam (Figure 4)
I_o	$t^3 / 12$ = moment of inertia per unit length
k	gauge distance from heel to the top of fillet (Figure 4)
l	length of the angle
M	connection moment
M_0	$\sigma_y t^2 / 4$ = plastic bending moment capacity per unit length
m	M / M_u
M_u	ultimate connection moment capacity
n	shape parameter of the three-parameter power model defined in Equation 16
R_k	tangent connection stiffness
R_{ki}	initial connection stiffness
V	shear force
V_o	$\delta_y t / 2$ = plastic shear capacity per unit length
t	angle thickness (Figure 4), subscripts w and t may be used to refer to web angle and top angle respectively
W	nut diameter (Figure 4)

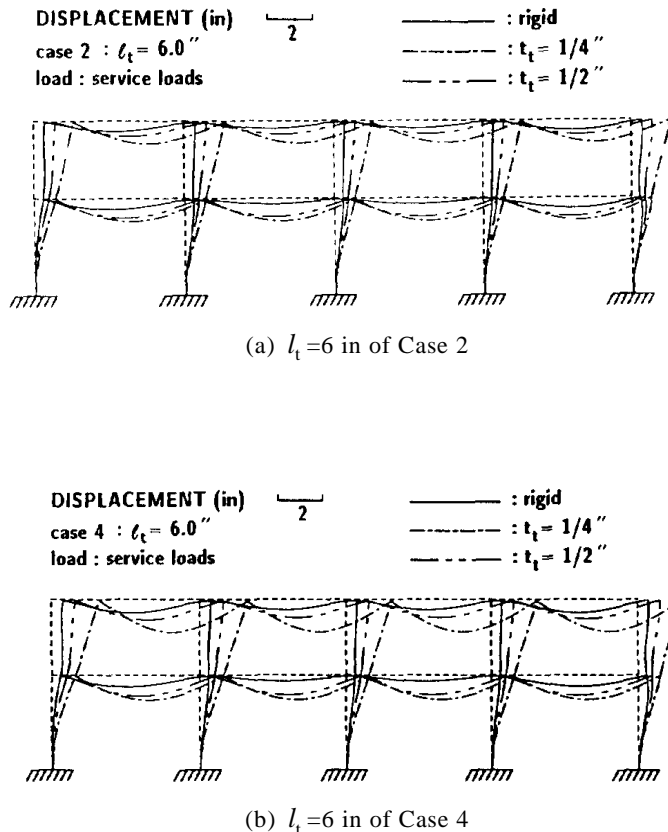
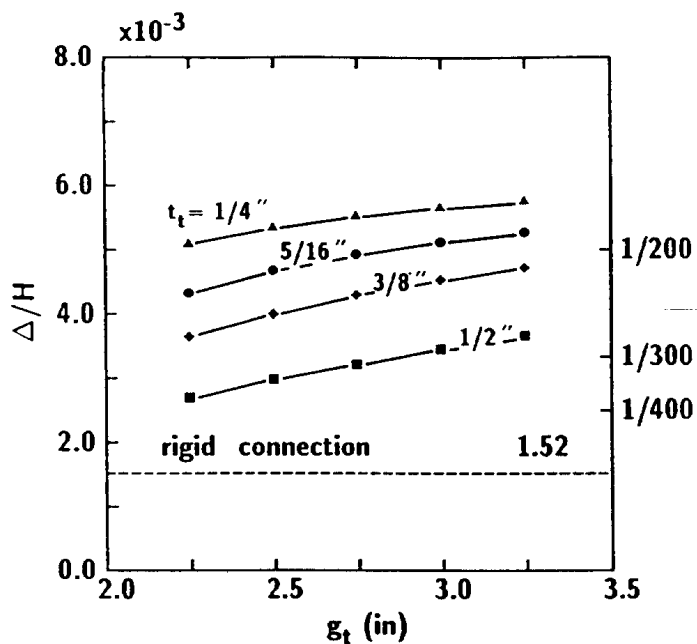
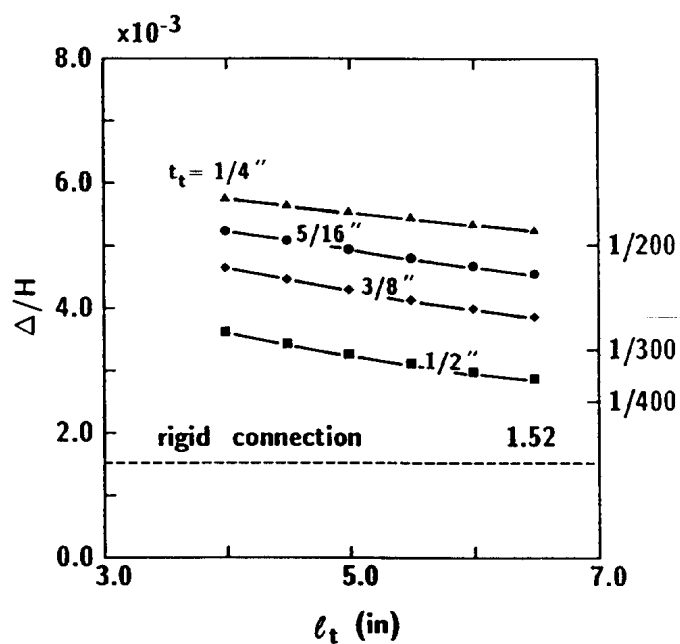


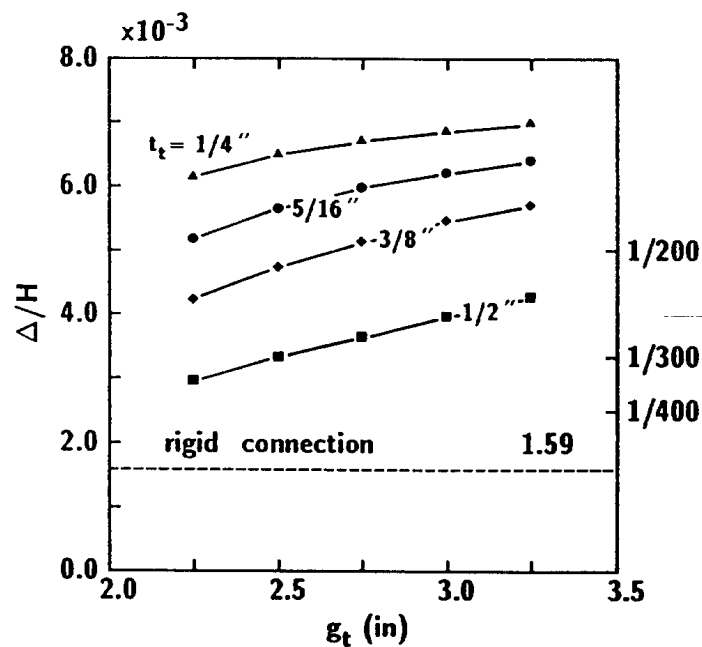
Fig. 16. General deformations of frame under service loads.



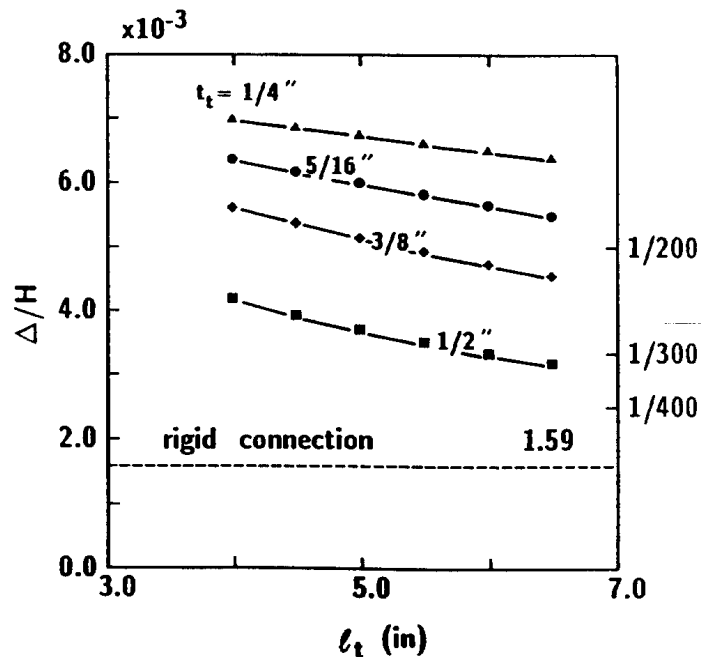
(a) Case 1



(b) Case 2



(c) Case 3

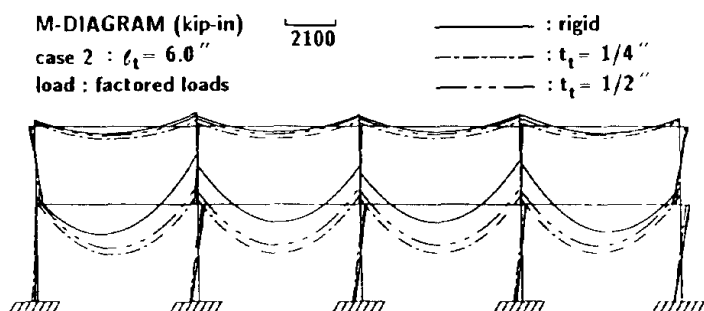


(d) Case 4

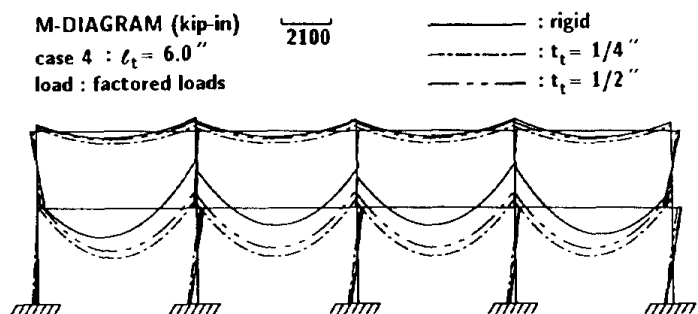
Fig. 17. Distributions of roof drift under service loads.

θ θ_r / θ_o
 θ_r relative rotation of connection
 θ_o M_u / R_{ki}
 ξ_w $V / V_o =$ non-dimensional ultimate shear force parameter in web angle
 ξ_t non-dimensional ultimate shear force parameter at the plastic hinge
 σ_y yield stress of steel
 β g / l

β_w' defined in Equation 3
 β_t^* defined in Equation 10
 β_t' defined in Equation 7
 γ l / t
 δ d / t
 κ k / t
 ω W / t
 ρ t_w / t_t



(a) $l_t = 6$ in of Case 2



(b) $l_t = 6$ in of Case 4

Fig. 18. Bending moment diagrams of frame under factored loads.

Table 3.
Non-dimensional End Moments of Columns
 $g_t = 2.5$ in. of Case 1

		T&S Angle with W Angle Connection				Rigid Connection			Reference Value (kip-in.)
Elment No.	Node No.	$t_t = 1/4$ -in.	$t_t = 5/16$ -in.	$t_t = 3/8$ -in.	$t_t = 1/2$ -in.	(1) Exact	B_1, B_2 Method		
							(2) Equation H1-5	(3) Equation H1-6	
1	1	3.00	2.74	2.44	1.91	1.16	1.22	1.33	-85.28
	2	-1.37	-1.10	-0.73	0.12	0.48	0.46	0.21	-32.46
2	4	1.39	1.33	1.26	1.15	1.06	1.08	1.12	-282.48
	5	0.61	0.64	0.67	0.73	1.06	1.07	1.11	297.07
3	7	1.54	1.47	1.39	1.27	1.07	1.07	1.12	-254.32
	8	0.74	0.77	0.82	0.88	1.07	1.07	1.12	242.04
4	10	1.68	1.61	1.53	1.39	1.07	1.07	1.12	-230.75
	11	0.91	0.96	1.01	1.09	1.10	1.07	1.13	195.40
5	13	1.18	1.17	1.18	1.19	1.05	1.03	1.06	-290.13
	14	0.60	0.68	0.77	0.95	1.03	1.02	1.04	379.62
6	2	0.50	0.62	0.75	0.95	1.00	1.00	1.00	301.11
	3	0.40	0.51	0.62	0.81	1.00	1.00	1.00	-252.37
7	5	0.26	0.20	0.16	0.18	1.01	1.01	1.01	-146.61
	6	0.84	0.89	0.93	0.97	1.02	1.01	1.01	125.05
8	8	0.60	0.44	0.32	0.29	1.01	1.02	1.01	-63.59
	9	1.56	1.64	1.68	1.61	1.02	1.02	1.02	66.26
9	11	-3.95	-2.84	-1.87	-1.07	0.90	0.88	0.88	9.81
	12	8.43	8.74	8.77	7.67	1.10	1.09	1.10	12.30
10	14	0.54	0.63	0.73	0.92	1.00	1.00	1.00	-367.51
	15	0.73	0.84	0.95	1.07	1.00	1.00	1.00	329.61

Table 3 (cont.).
Non-dimensional End Moments of Columns
 $t_t = 3/8$ -in. of Case 2

		T&S Angle with W Angle Connection						Rigid Connection			Reference Value (kip-in.)
Elment No.	Node No.	$l_t = 4.0$ in.	$l_t = 4.5$ in.	$l_t = 5.0$ in.	$l_t = 5.5$ in.	$l_t = 6.0$ in.	$l_t = 6.5$ in.	(1) Exact	B_1, B_2 Method		
									(2) Equation H1-5	(3) Equation H1-6	
1	1	2.73	2.65	2.58	2.51	2.44	2.38	1.16	1.22	1.33	−85.28
	2	−1.07	−0.99	−0.90	−0.81	−0.73	−0.64	0.48	0.46	0.21	−32.46
2	4	1.33	1.31	1.29	1.28	1.26	1.25	1.06	1.08	1.12	−282.48
	5	0.64	0.65	0.65	0.66	0.67	0.68	1.06	1.07	1.11	297.07
3	7	1.46	1.44	1.43	1.41	1.39	1.38	1.07	1.07	1.12	−254.32
	8	0.78	0.79	0.80	0.81	0.82	0.82	1.07	1.07	1.12	242.04
4	10	1.61	1.58	1.56	1.55	1.53	1.51	1.07	1.07	1.12	−230.75
	11	0.96	0.97	0.99	1.00	1.01	1.02	1.10	1.07	1.13	195.40
5	13	1.18	1.18	1.17	1.17	1.18	1.18	1.05	1.03	1.06	−290.13
	14	0.68	0.70	0.73	0.75	0.77	0.79	1.03	1.02	1.04	379.62
6	2	0.63	0.67	0.70	0.73	0.75	0.78	1.00	1.00	1.00	301.11
	3	0.52	0.55	0.58	0.60	0.62	0.65	1.00	1.00	1.00	−252.37
7	5	0.19	0.18	0.17	0.16	0.16	0.15	1.01	1.01	1.01	−146.61
	6	0.89	0.90	0.91	0.92	0.93	0.94	1.02	1.01	1.01	125.05
8	8	0.42	0.39	0.36	0.33	0.32	0.30	1.01	1.02	1.01	−63.59
	9	1.64	1.66	1.67	1.68	1.68	1.69	1.02	1.02	1.02	66.26
9	11	−2.74	−2.48	−2.24	−2.04	−1.87	−1.73	0.90	0.88	0.88	9.81
	12	8.75	8.79	8.80	8.80	8.77	8.72	1.10	1.09	1.10	12.30
10	14	0.63	0.66	0.68	0.70	0.73	0.75	1.00	1.00	1.00	−367.51
	15	0.85	0.88	0.91	0.93	0.95	0.97	1.00	1.00	1.00	329.61

Table 3.
Non dimensional End Moments of Columns
 $g_t = 2.5$ in. of Case 3

		T&S Angle with W Angle Connection				Rigid Connection			Reference Value (kip-in.)
Elment No.	Node No.	$t_t = 1/4$ -in.	$t_t = 5/16$ -in.	$t_t = 3/8$ -in.	$t_t = 1/2$ -in.	(1) Exact	B_1, B_2 Method		
							(2) Equation H1-5	(3) Equation H1-6	
1	1	3.49	3.16	2.79	2.10	1.18	1.25	1.37	-78.31
	2	-0.66	-0.49	-0.25	0.34	0.64	0.63	0.45	-48.26
2	4	1.46	1.39	1.31	1.17	1.06	1.08	1.13	-284.67
	5	0.55	0.59	0.63	0.70	1.06	1.07	1.11	299.00
3	7	1.62	1.54	1.45	1.29	1.07	1.07	1.12	-255.26
	8	0.68	0.73	0.78	0.86	1.07	1.07	1.12	241.40
4	10	1.78	1.69	1.59	1.42	1.07	1.07	1.12	-230.72
	11	0.85	0.91	0.97	1.08	1.10	1.07	1.14	192.74
5	13	1.21	1.20	1.19	1.19	1.05	1.03	1.06	-297.85
	14	0.55	0.63	0.73	0.93	1.03	1.02	1.04	392.94
6	2	0.39	0.53	0.68	0.92	1.00	1.00	1.00	330.36
	3	0.44	0.54	0.65	0.82	1.00	1.00	1.00	-291.10
7	5	0.46	0.36	0.27	0.22	1.02	1.01	1.01	-151.84
	6	0.65	0.74	0.84	0.97	1.02	1.01	1.00	121.47
8	8	1.02	0.79	0.56	0.37	1.02	1.02	1.02	-66.24
	9	1.20	1.36	1.51	1.61	1.03	1.02	1.02	64.67
9	11	-7.00	-5.37	-3.66	-1.67	0.92	0.88	0.90	9.54
	12	6.40	7.18	7.83	7.58	1.08	1.08	1.07	12.11
10	14	0.56	0.64	0.73	0.91	1.00	1.00	1.00	-398.34
	15	0.63	0.75	0.88	1.03	1.00	1.00	1.00	363.95

Table 3 (cont.).
Non-dimensional End Moments of Columns
 $t_t = \frac{3}{8}$ -in. of Case 2

		T&S Angle with W Angle Connection						Rigid Connection			Reference Value (kip-in.)
Elment No.	Node No.	$l_t = 4.0$ in.	$l_t = 4.5$ in.	$l_t = 5.0$ in.	$l_t = 5.5$ in.	$l_t = 6.0$ in.	$l_t = 6.5$ in.	(1) Exact	B_1, B_2 Method		
									(2) Equation H1-5	(3) Equation H1-6	
1	1	3.15	3.06	2.96	2.88	2.79	2.71	1.18	1.25	1.37	−78.31
	2	−0.47	−0.42	−0.36	−0.30	−0.25	−0.19	0.64	0.63	0.45	−48.26
2	4	1.39	1.37	1.34	1.33	1.31	1.29	1.06	1.08	1.13	−284.67
	5	0.59	0.60	0.61	0.62	0.63	0.64	1.06	1.07	1.11	299.00
3	7	1.53	1.51	1.49	1.47	1.45	1.43	1.07	1.07	1.12	−255.26
	8	0.73	0.74	0.75	0.77	0.78	0.79	1.07	1.07	1.12	241.40
4	10	1.69	1.66	1.64	1.62	1.59	1.57	1.07	1.07	1.12	−230.72
	11	0.91	0.93	0.94	0.96	0.97	0.99	1.10	1.07	1.14	192.74
5	13	1.20	1.19	1.19	1.19	1.19	1.19	1.05	1.03	1.06	−297.85
	14	0.64	0.66	0.69	0.71	0.73	0.75	1.03	1.02	1.04	392.94
6	2	0.54	0.58	0.61	0.65	0.68	0.71	1.00	1.00	1.00	330.36
	3	0.55	0.57	0.60	0.62	0.65	0.67	1.00	1.00	1.00	−291.10
7	5	0.35	0.33	0.30	0.28	0.27	0.25	1.02	1.01	1.01	−151.84
	6	0.75	0.77	0.79	0.82	0.84	0.85	1.02	1.01	1.00	121.47
8	8	0.77	0.71	0.66	0.61	0.56	0.52	1.02	1.02	1.02	−66.24
	9	1.37	1.41	1.45	1.48	1.51	1.53	1.03	1.02	1.02	64.67
9	11	−5.24	−4.80	−4.38	−4.00	−3.66	−3.35	0.92	0.88	0.90	9.54
	12	7.22	7.42	7.58	7.72	7.83	7.91	1.08	1.08	1.07	12.11
10	14	0.64	0.67	0.69	0.71	0.73	0.75	1.00	1.00	1.00	−398.34
	15	0.77	0.80	0.83	0.86	0.88	0.91	1.00	1.00	1.00	363.95